

ANL/CP--72644

DE91 011166

(CONF-910199--)

The submitted manuscript has been authored by a contractor of the U.S. Government under contract No. W-31-109-ENG-38. Accordingly, the U.S. Government retains a nonexclusive, royalty-free license to publish or reproduce the published form of this contribution, or allow others to do so, for U.S. Government purposes.
--

2-D AND 3-D COMPUTATIONS OF CURVED ACCELERATOR MAGNETS*

Larry R. Turner
Accelerator Systems Division, Advanced Photon Source
Argonne National Laboratory, Argonne, Illinois 60439, USA

Abstract: In order to save computer memory, a long accelerator magnet may be computed by treating the long central region and the end regions separately. The dipole magnets for the injector synchrotron of the Advanced Photon Source (APS), now under construction at Argonne National Laboratory (ANL), employ magnet iron consisting of parallel laminations, stacked with a uniform radius of curvature of 33.379 m. Laplace's equation for the magnetic scalar potential has a different form for a straight magnet (x - y coordinates), a magnet with surfaces curved about a common center (r - θ coordinates), and a magnet with parallel laminations like the APS injector dipole. Yet pseudo 2-D computations for the three geometries give basically identical results, even for a much more strongly curved magnet. Hence 2-D (x - y) computations of the central region and 3-D computations of the end regions can be combined to determine the overall magnetic behavior of the magnets.

Introduction

For the foreseeable future, the accuracy of three-dimensional (3-D) magnet computations will be limited by the number of elements and nodes that can be computed with the available computer memory. Consequently it is desirable that the entire geometry of long magnets not be included in the computation, but only the end regions, with the contribution of the central region to be added from two-dimensional (2-D) calculations. This paper addresses that possibility for long curved accelerator magnets.

The particular magnet considered here is the dipole for the injector synchrotron of the Advanced Photon Source (APS) now under construction at Argonne National Laboratory (ANL). Figure 1. shows a cross sectional view of the synchrotron dipole. In the longitudinal (beam) direction, the magnet iron consists of parallel laminations, stacked with a uniform radius of curvature of 33.379 m. The sides of the racetrack coils have that same curvature, and the two straight ends of each coil are parallel.

Pseudo 2-D Computations

That geometry does not correspond to either of the two, x - y or r - θ ,

*Work supported by U.S. Department of Energy, Office of Basic Energy Sciences under Contract No. W-31-109-ENG-38.

MASTER

DISTRIBUTION OF THIS DOCUMENT IS UNLIMITED

normally treated in 2-D. For the three geometries, Laplace's equation for the potential V may be written:

$$\frac{\partial^2 V}{\partial x^2} + \frac{\partial^2 V}{\partial y^2} = 0 \quad \text{x-y} \quad (1)$$

$$\frac{\partial^2 V}{\partial r^2} + \frac{1}{r} \frac{\partial V}{\partial r} + \frac{\partial^2 V}{\partial y^2} = 0 \quad \text{r-}\theta \quad (2)$$

$$\frac{\partial^2 V}{\partial w^2} + \frac{1}{R} \frac{\partial V}{\partial w} + \frac{\partial^2 V}{\partial y^2} = 0 \quad \text{parallel} \quad (3)$$

Equation 3 is found as follows. For the parallel geometry, we approximate the circular arc with a sinusoidal one, and write $V = V(w, y)$ where

$$w = x + a [1 - \cos(kz)]. \quad (4)$$

After differentiating in x, y, and z, we take the limit $\cos(kz) = 1$,

$$\sin^2(kz) = 0,$$

and we set $ak^2 = 1/R$, where R is the fixed radius of curvature.

Equations (1) - (3) were not solved directly. Instead pseudo 2-D computations were run for the synchrotron dipole for all three geometries with the 3-D magnetostatics code TOSCA [1]. Figure 2 shows the coil and iron geometries. For each geometry the cross section was held the same over a 200 mm length, and a no flux crossing boundary condition was applied at each end. That assured that the field had no component in the third dimension, and did not vary in that direction. To make the results more sensitive to the curvature, the radius of curvature for the r- θ and parallel geometries was taken ten times smaller than the true value (3.3379 m rather than 33.379 m). For the parallel geometry, x varied with z to give the correct curvature, but the two ends were parallel. For the r- θ geometry, the two end planes each contained the center of curvature. In each case, a pair of coils of the appropriate geometry was used.

For the x-y and r- θ cases, reflections at the ends continued the geometry correctly, but reflections caused a slope discontinuity for the parallel case. Comparing results for different lengths showed that this discontinuity did not degrade the computed fields.

Figure 3 shows that the contour plots of B_y across the beam region did not vary for the three cases, even though the curvature was ten times too large.

3-D Computations for a Short Magnet

The above results show that it should be acceptable to do a 3-D computation for the end region only, and treat the central region through the results of an x-y 2-D computation. Figure 4 shows how the short magnet is created from the long, and Fig. 5 shows the TOSCA geometry. Both unbeveled and beveled ends were computed.

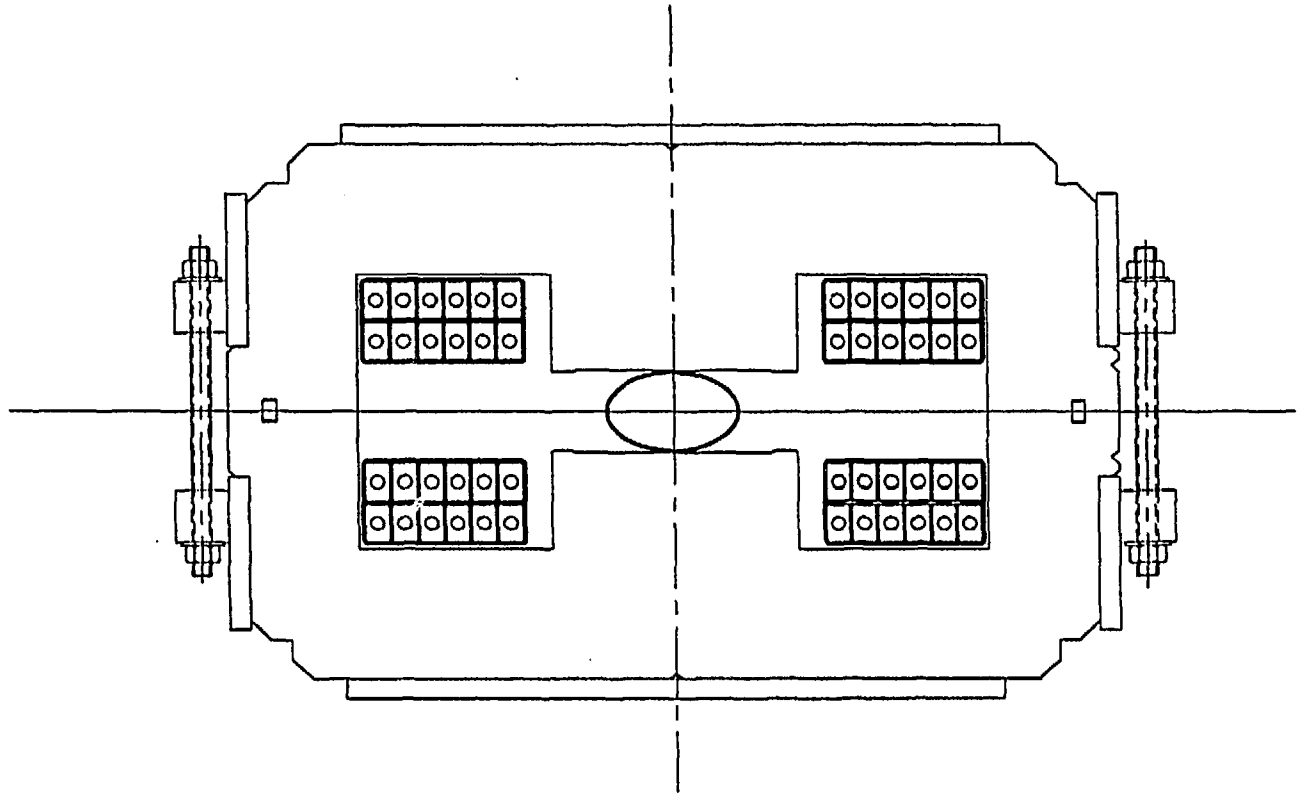
The 3-D analysis yields the effective length of the magnet, defined as the integral of the field component B_y through the magnet in the beam direction z , and also shows how the effective length varies with horizontal displacement x of the beam. From Fig. 4 it can be seen that the variation can be found from integration along the paths shown for the short magnet. All paths have the same length inside the magnet, and all have the same length outside. Figure 6 shows the difference between the effective length of the magnet and the length of the iron as a function of horizontal position across the magnet gap. Results for both straight vertical steel pole ends and beveled pole ends are shown. Positive or negative curvature of the plots correspond to opposite signs of the sextupole component of the integrated field through the magnet.

References

[1] Available from Vector Fields Ltd, Oxford, UK.

DISCLAIMER

This report was prepared as an account of work sponsored by an agency of the United States Government. Neither the United States Government nor any agency thereof, nor any of their employees, makes any warranty, express or implied, or assumes any legal liability or responsibility for the accuracy, completeness, or usefulness of any information, apparatus, product, or process disclosed, or represents that its use would not infringe privately owned rights. Reference herein to any specific commercial product, process, or service by trade name, trademark, manufacturer, or otherwise does not necessarily constitute or imply its endorsement, recommendation, or favoring by the United States Government or any agency thereof. The views and opinions of authors expressed herein do not necessarily state or reflect those of the United States Government or any agency thereof.



SYNCHROTRON DIPOLE CROSS SECTION

Figure 1. Cross section of the dipole magnet for the APS injector synchrotron.

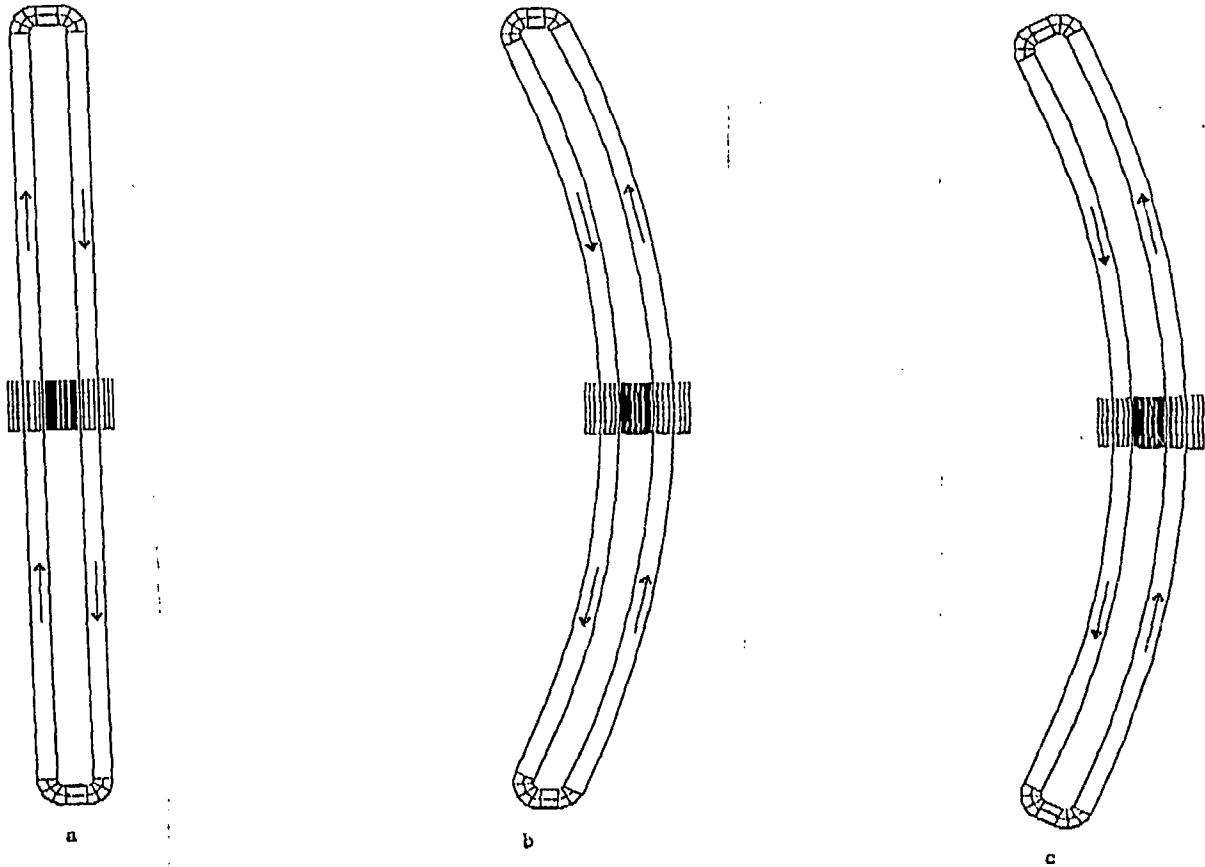


Figure 2. Geometries for the three coordinate cases: (a) $x-y$, (b) parallel, (c) $r-\theta$. In each case, the full length coil and a short section of iron, with appropriate boundary conditions is shown.

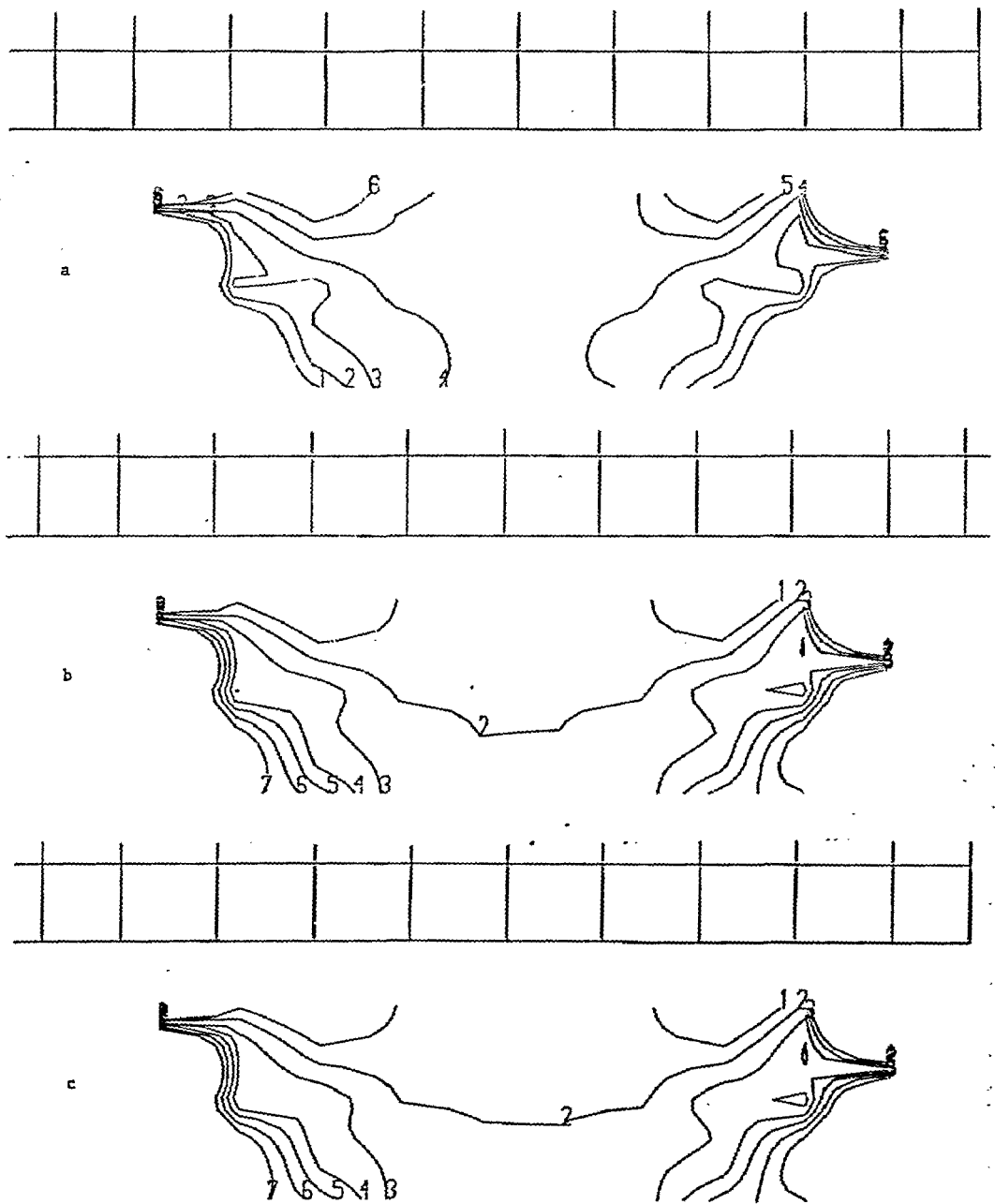
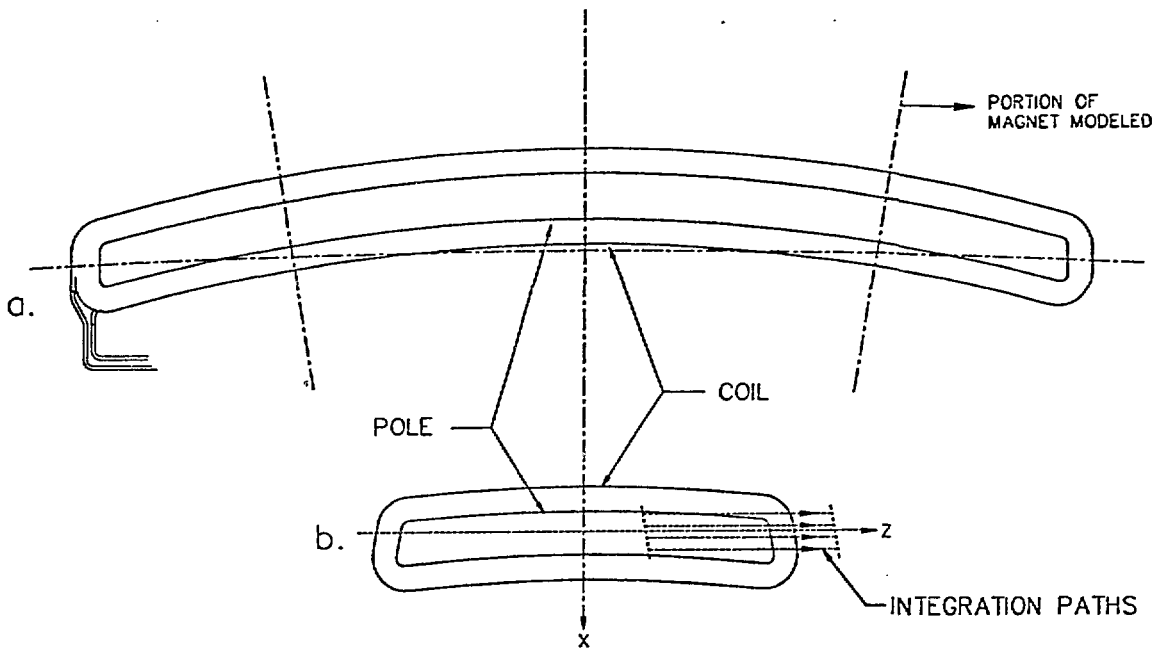


Figure 3. Contour plots of B_y for the three pseudo 2-D computations. X: -20 to 20mm. Y: 0 to 15mm. Contour spacing is $0.5G$ ($5 \times 10^{-4}T$). (a) x-y, (b) parallel, (c) r- θ .



- a. TRUE GEOMETRY OF LONG DIPOLE MAGNET.
 b. GEOMETRY USED FOR COMPUTATION.

Figure 4. How the ends of the long magnet are modeled as a short magnet. (a) True geometry of the long magnet. (b) geometry used for computation.

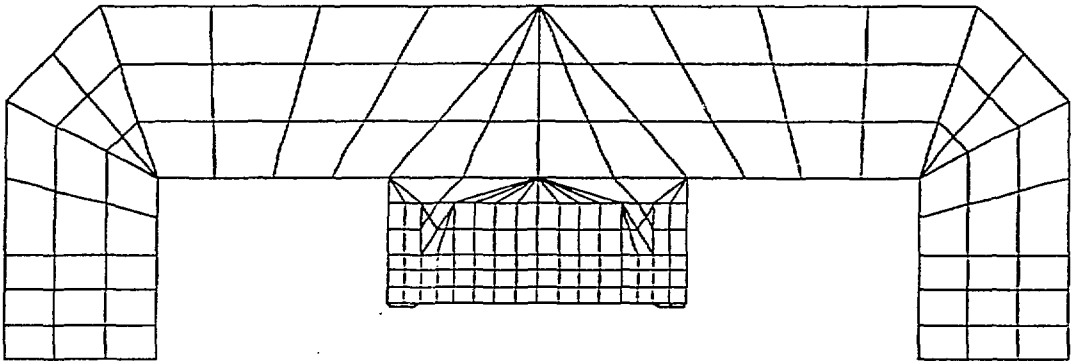
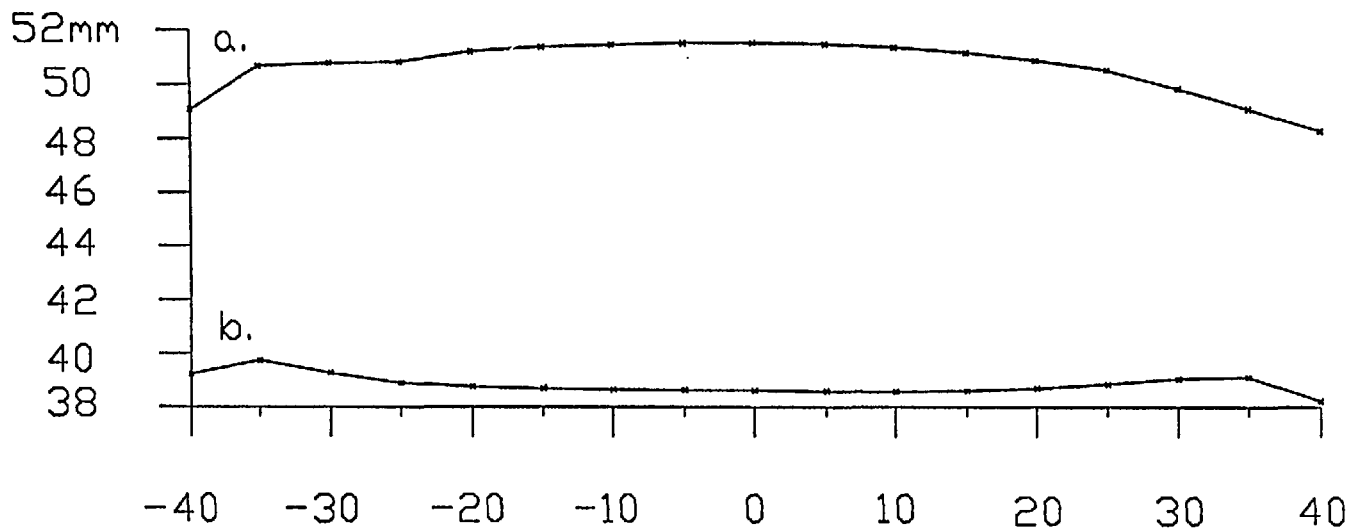


Figure 5. TOSCA model for the injector synchrotron dipole magnet, iron only.



SYNCHROTRON DIPOLE
EFFECTIVE LENGTH—STEEL LENGTH

Figure 6. Plot of effective length against horizontal position in the magnet gap, for (a) straight and (b) beveled pole ends. The difference between effective length and steel length is shown.